International Journal of Microwave and Wireless Technologies

cambridge.org/mrf

Transmission line approach of zero-index metamaterials and applications using a wave concept iterative method

Mohamed Karim Azizi[1], Taieb Elbellili[1], Henri Baudrand[2] and Hichem Trabelsi[1]

[1]Unit of Research Circuits and Electronics Systems High Frequency, Faculté des Sciences, Université El Manar, Tunis, Tunisia and [2]Laplace Lab, Department of Electronics, Faculty ENSEEIHT, University of Toulouse, Toulouse, France

Research Paper

Cite this article: Karim Azizi M, Elbellili T, Baudrand H, Trabelsi H (2019). Transmission line approach of zero-index metamaterials and applications using a wave concept iterative method. *International Journal of Microwave and Wireless Technologies* **11**, 244–254. https://doi.org/10.1017/S175907871800168X

Received: 28 March 2018
Revised: 8 December 2018
Accepted: 10 December 2018
First published online: 7 February 2019

Key words:
2-D transmission line metamaterials; electromagnetic field distribution; metamaterials; WCIP; zero-refractive index-metamaterials

Author for correspondence:
Mohamed Karim Azizi,
E-mail: medkarim.azizi@gmail.com

Abstract

In this paper, we propose a novel study of zero-index materials (ZIM) based on lumped element circuits using a wave concept iterative method (WCIP). This method is well used to demonstrate the behavior of zero-index-based microwave applications. This type of metamaterial can maintain the amplitude and the phase of an electromagnetic wave to be constant through the ZIM region, which is an important property to design an in-phase power divider-combiner, enhance the directivity of an embedded source, channel electromagnetic waves without reflection at the interface between waveguides with different cross-sections, and control the transmission of electromagnetic wave by the adjustment of the permittivity of a dielectric defect coated by zero-index metamaterial. The numerical simulations using the WCIP method match the literature and commercial software simulator results.

Introduction

Metamaterials, as artificial materials which have unusual properties, have been largely reported in the literature [1–6]. Metamaterials with effective constitutive parameters can be synthesized using lumped element circuits or lumped element-loaded microstrip transmission lines. Recently, there have been many works concerning an important class of metamaterials called zero-index materials (ZIM) whose permittivity and (or) permeability are equal to zero. ZIM can be used for a wide range of applications, such as the enhancement of the directivity of an electromagnetic source located in ZIM medium [7], the tunneling of the electromagnetic wave through a narrow cross section waveguide [8–11], and the control of the transmission of electromagnetic energy by defects loaded ZIM waveguides [12,13]. The above works have studied ZIM analytically by the resolution of Maxwell's equations and carrying out numerical simulations using the finite element-based COMSOL Multiphysics software without discussing the physical realization of these ZIM-based applications. Moreover, it is difficult to experimentally synthesize ZIM with simultaneously zero permittivity and zero permeability to assure a perfect matching between ZIM medium and conventional medium. However, the fabrication of metamaterials presenting only one effective parameter permittivity or permeability equal to zero is less challenging than those presenting two effective parameters equal to zero at the same time.

The physical implementation of ZIM given in the literature [14–16] is based on non-compact and resonant circuits using split ring resonators. As a solution to the quoted limits, we study, in this paper, how to implement ZIM with simultaneously effective permittivity and permeability equal to zero in order to abide by the matching condition between the different parts constituting the periodic circuit by using transmission lines loaded with the lumped elements capacitors and inductors. The use of this approach permits the design of ZIM by choosing a resonant frequency everywhere over a wide bandwidth by simply tuning the values of inductors and capacitors because the bandwidth of metamaterial transmission line is only limited by the cut-off frequencies of their LC–CL equivalent models. Also, we can obtain a compact circuit since it is implemented using transmission lines where the constitutive basic unit cell is much smaller than the guided wavelength at the operating frequency. Moreover, we give more flexibility to choose the resonant frequency required when designing ZIM.

Metamaterial transmission line circuits can be treated as periodic circuits in either 1-D or 2-D configurations. As a consequence, we can easily and effectively model continuous media with arbitrary and effective given material parameters. In addition, we can really describe the behavior of these periodic circuits by showing the spatial distribution of the electromagnetic field by calculating the field parameters at each node of the periodic circuit.

Another challenge is to perfectly choose a numerical method of simulation which guarantees an easy and fast analysis of the electromagnetic problem. In the literature, transmission line matrix (TLM) and transmission matrix method (TMM) methods [17–19] are specially

CAMBRIDGE UNIVERSITY PRESS

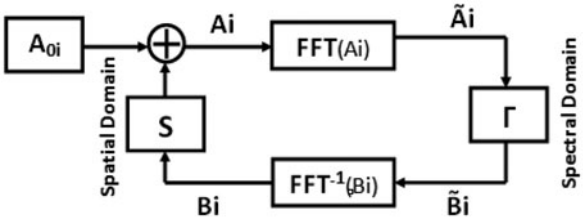

Fig. 1. The iterative wave diagram.

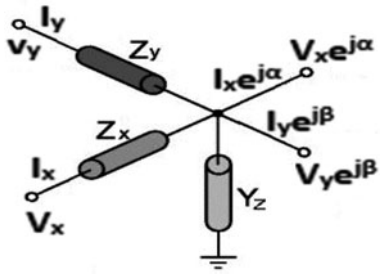

Fig. 2. A basic unit cell of a periodic transmission line circuit.

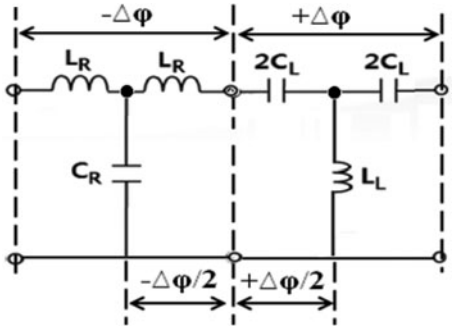

Fig. 3. Combination of RH/LH unit cells with opposite insertion phases.

used to analyze periodic lumped circuits. These methods have remarkable limits such as complex programing of the parameters of the periodic circuits which largely differs from one circuit to other and the problem of stability when manipulating very large circuits.

The use of commercial software is not usually the best solution because they also have their specific limits. Some commercial software are designed to perform an electromagnetic field simulation such as HFSS and COMSOL Multiphysics which are based on the finite element method (FEM). FEM method requires a lot of simulation time and big memory. Although Advanced Design System (ADS) software can permit lumped circuit simulations, it requires the labeling of all nodes of the periodic circuit where we intend to calculate voltage and current to show the electromagnetic field distributions. The labeling of nodes is very difficult to achieve in the case of very large periodic circuits.

To overcome all the above requirements, we use a wave concept iterative method (WCIP) which has been recently used to accurately analyze both 1-D and 2-D metamaterial periodic lumped circuits [20–28].

In this work, we first explain how to combine right-handed (RH) and left-handed (LH) unit cells to synthesize a continuous medium with simultaneously zero permittivity and permeability called zero-index medium. Second, we demonstrate some zero-index transmission line microwave-based applications, numerically by using the WCIP method, concerning the enhancement of the directivity of an electromagnetic source embedded in a ZIM region, the coherent power combination of many arbitrary located electromagnetic sources, and the control of the electromagnetic wave transmission using waveguides loaded with ZIM. Finally, we finish with a conclusion.

The basic theory of the WCIP method and synthesis of zero refractive index materials

The basic theory of the WCIP method

The iterative method WCIP is well used to study the behavior of metamaterial circuits, such as lenses [20] where a periodic circuit can be established around RH/LH unit cells to synthesize positive and negative refractive index media, respectively. In the same reference, the WCIP method is used to analyze arbitrary shaped periodic lumped circuits, which proves that the proposed method gives more flexibility to design and study metamaterial circuits. This method based on the concept of waves directly gives the voltage and the current at each node of the periodic circuit. As a consequence, we can show the behavior of many metamaterial devices by just visualizing the spatial distribution of voltage and current as equivalent distributions of electric and magnetic fields. The parameters manipulated by the iterative process are basically the incident waves $A/\tilde{A}$ and reflected waves $B/\tilde{B}$ in spatial/spectral domains. The passage between the two domains is done iteratively by the application of a fast Fourier transform (FFT) and its inverse (FFT^{-1}) until the convergence of the iterative process is reached. The iterative process is just based on two equations (1) according to the diagram depicted by Fig. 1:

$$\begin{cases} A_i = SB_i + A_{0_i} & \text{spatial domain} \\ \tilde{B}_i = \Gamma\tilde{A}_i & \text{spectral domain} \end{cases} \quad (1)$$

A_i/B_i and $\tilde{A}_i/\tilde{B}_i$ are the incident/reflected waves in the spatial and the spectral domains at the ith iteration, respectively. S is the spatial reflection coefficient calculated at each axis (X, Y, and Z) of each unit cell. Γ is the spectral reflection operator calculated at each unit cell and A_0 is the source's excitation wave.

The diagram given in Fig. 1 identifies the different waves presented in the iterative process.

Since we use the iterative method to study periodic circuits, the calculation of S and Γ will be done over one basic unit cell, as depicted in Fig. 2 where the series impedance and shunt admittance will take the lumped elements inductor and capacitor.

Based on the system of equations (1), the running of the WCIP process just requires the determination of the spatial and the spectral operators S and Γ at each unit cell.

The spatial reflection coefficient is given by [20] as follows:

$$S_\Delta = \frac{Z_\Delta - Z_0}{Z_\Delta + Z_0} \quad (2)$$

where Z_Δ is the impedance along the axis $\Delta = (X, Y, Z)$ and Z_0 is the characteristic impedance.

Whereas, the spectral reflection operator is written as follows:

$$\Gamma = \frac{1 - Z_0\bar{Y}}{1 + Z_0\bar{Y}} \quad (3)$$

https://doi.org/10.1017/S175907871800168X Published online by Cambridge University Press

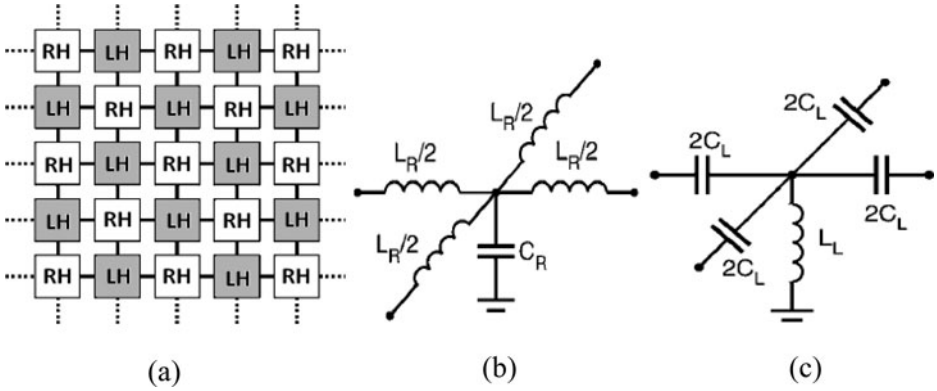

Fig. 4. (a) Illustration of 2-D ZIM medium by alternating between RH and LH unit cells, (b) RH unit cell, and (c) LH unit cell.

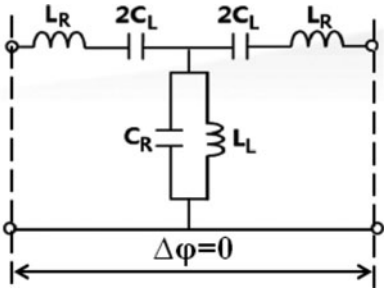

Fig. 5. CRLH unit cell at the operating frequency ω_0.

where $\bar{Y}$ is the admittance matrix which relates currents and voltages over one unit cell [20].

After the convergence of the iterative process, we can directly find the voltage and current at each node by using the following equations:

$$\begin{cases} V_{x,y,z} = \sqrt{Z_0}(A_{x,y,z}(i,j) + B_{x,y,z}(i,j)) \\ I_{x,y,z} = \dfrac{1}{\sqrt{Z_0}}(A_{x,y,z}(i,j) - B_{x,y,z}(i,j)) \end{cases} \tag{4}$$

Synthesis of zero-index materials

The phase velocity $V\varphi$ in a medium with an index of refraction n is given by

$$V\phi = \frac{c}{n} \tag{5}$$

where c is the speed of light in vacuum.

If the index of refraction tends to zero, the phase velocity will be infinite which gives an infinite guided wavelength according to the following expression:

$$\lambda_g = \frac{V\phi}{f} \tag{6}$$

An infinite guided wavelength can be explicated by a constant phase and no amplitude variation. The combination of materials which have opposite phase constants can be used to generate ZIM media. Thus, we can combine RH and LH unit cells to have a total insertion phase equal to zero over a very small length.

Figure 3 shows the combination of two RH/LH unit cells with opposite insertion phases.

A tessellated 2-D RH/LH medium is considered as a ZIM medium, as depicted in Fig. 4(a).

To avoid any reflection of electromagnetic energy, RH/LH unit cells should be matched to the same characteristic impedance. So, we should have the equality expressed as the follows:

$$Z_C = \sqrt{\frac{L_R}{C_R}} = \sqrt{\frac{L_L}{C_L}} \tag{7}$$

We can deduce the same equality as follows:

$$L_R C_L = L_L C_R \tag{8}$$

Also, RH/LH unit cells should have the same absolute values of their insertion phases. Given by the following equations (9)

$$\begin{aligned} \Delta\phi_{RH} &= \beta_{RH}\Delta l = \omega\sqrt{L_R C_R} \\ \Delta\phi_{LH} &= \beta_{LH}\Delta l = -\frac{1}{\omega\sqrt{L_L C_L}} \end{aligned} \tag{9}$$

The equality $\Delta\varphi_{RH} = \Delta\varphi_{LH}$ leads to the following equation:

$$\omega_0^2\sqrt{L_R C_R L_L C_L} = 1 \tag{10}$$

Using (8) and (10), we can write

$$\omega_0^2 = \frac{1}{\sqrt{L_R C_L}\sqrt{L_L C_R}} \tag{11}$$

Equation (11) leads to

$$\omega_0 = \frac{1}{\sqrt{L_R C_L}} = \frac{1}{\sqrt{L_L C_R}} \tag{12}$$

At the operating frequency ω_0, we can deduce from (12) that the series inductance L_R of the RH unit cell resonates with the series capacitance C_L of the LH unit cell, whereas the shunt elements C_R and L_L resonate together. Therefore, the overall combined RH/LH unit cells behave as there is no phase shift along it. The novel unit cell is called CRLH (composite right left handed) unit cell [29] with zero insertion phase as depicted in Fig. 5.

https://doi.org/10.1017/S175907871800168X Published online by Cambridge University Press

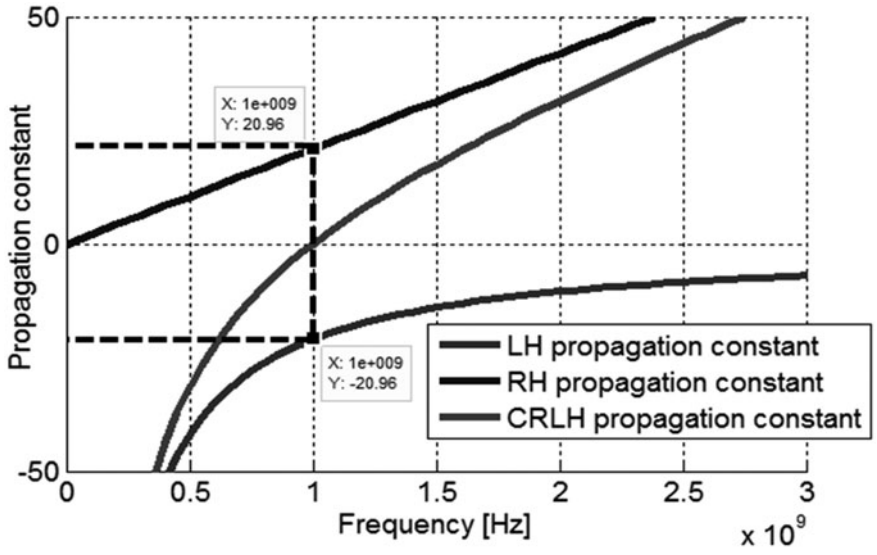

Fig. 6. Variation of the constant of propagation according to the frequency.

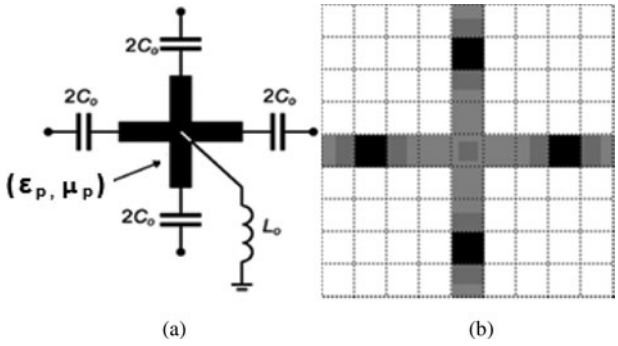

Fig. 7. A CRLH unit cell which uses microstrip lines loaded with lumped capacitor and inductor: (a) microstrip/lumped element model and (b) layout model.

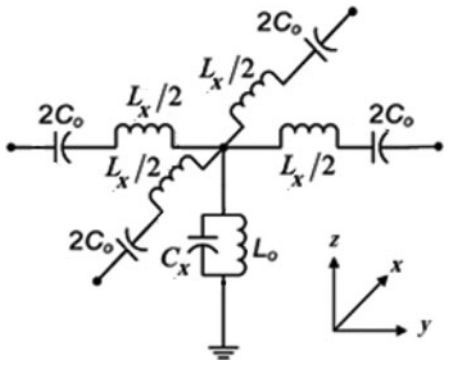

Fig. 8. Equivalent lumped element CRLH unit cell.

The series resonant frequency ω_{se} of the series branch and the shunt resonant frequency ω_{sh} of the shunt branch are given by the following equations:

$$\omega_{se} = \frac{1}{\sqrt{L_R C_L}}$$
$$\omega_{sh} = \frac{1}{\sqrt{L_L C_R}} \quad (13)$$

At $f_0 = 1$ GHz, the propagation constant $\beta = 2\pi/\lambda$ is equal to zero (Fig. 6) which signifies that λ tends to the infinity. Since, the wavelength is infinite, the phase and the amplitude of the wave propagating through the region implemented by CRLH unit cell are independent of the position. So, we talk about a medium of zero-refractive index, as explained above.

The CRLH unit cell can be implemented using hybrid microstrip-lumped elements technology, as depicted in Fig. 7. The design of an effective continuous medium using the CRLH unit cell requires that its physical length should be much smaller than the guided wavelength.

Figure 7 shows the layout of the CRLH unit cell using microstrip transmission lines loaded with the lumped elements inductor L_0 and capacitor C_0.

We can express the effective permittivity and permeability of a medium manufactured with the previous proposed implementation of the CRLH unit cell as a function of the intrinsic material parameters ε_p and μ_p of the host microstrip transmission line and the loading lumped elements L_0 and C_0 [30] as follows:

$$\varepsilon_{eff}(\omega) = \varepsilon_p - \frac{g}{\omega^2 L_0 \Delta l}$$
$$\mu_{eff}(\omega) = \mu_p - \frac{1/g}{\omega^2 C_0 \Delta l} \quad (14)$$

where the structural factor g of the transmission line is defined as the ratio between the characteristic impedance and the effective wave impedance of the host transmission line:

$$g = \frac{Z_0}{\eta_{eff}} \quad (15)$$

Figure 8 shows an equivalent lumped element representation of the CRLH unit cell given in Fig. 7 where L_x and C_x represent the per-unit-length inductance and per-unit-length capacitance of the host RH transmission line.

According to the equivalent lumped element CRLH unit cell, we can write the effective permittivity and permeability

https://doi.org/10.1017/S175907871800168X Published online by Cambridge University Press

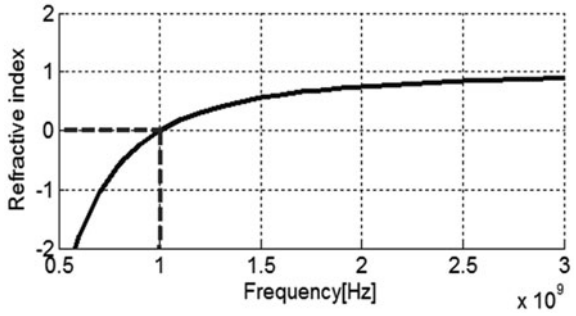

Fig. 9. Variation of the refractive index for CRLH unit cell according to the frequency (C_R = 88.5 fF, C_L = 2.0 pF, L_R = 12.5 nH, L_L = 286 nH).

as a function of the lumped elements L_x/L_0 and C_x/C_0 as follows [29]:

$$\varepsilon_{eff}(\omega) = g\left(C_x - \frac{1}{\omega^2 L_0 \Delta l}\right)$$
$$\mu_{eff}(\omega) = \left(L_x - \frac{1}{\omega^2 C_0 \Delta l}\right)/g \tag{16}$$

Let us consider the RT/Duroid 5880 substrate with permittivity relative $\varepsilon_r = 2.2$ and a thickness h of 1.575 mm. So, we can derive a width w of 1.39 mm for a 100 Ω host transmission line.

The structural transmission line factor g as a function of the width w and the thickness h of the substrate is given by [31] as follows:

$$g = \frac{1}{2\pi}\ln\left(\frac{8h}{w} + \frac{w}{4h}\right) \tag{17}$$

Equating between (14) and (16), the per-unit-length capacitance C_x and inductance L_x are then given by

$$C_x = \frac{\varepsilon_0 \varepsilon_{r_{eff}}}{g}$$
$$L_x = \mu_0 g \tag{18}$$

The calculated values of L_x and C_x are 43.99 nF/m and 444.4 nH/m.

For a zero values of both effective permittivity and permeability, the loading lumped elements L_0 and C_0 are given by

$$L_0 = \frac{1}{\omega_0^2 C_x \Delta l}$$
$$C_0 = \frac{1}{\omega_0^2 L_x \Delta l} \tag{19}$$

An RH unit cell of length Δl = 10 mm at 1 GHz gives L_0 and C_0 equal to 57.5 nH and 5.7 pF, respectively.

According to equations (9), the insertion phase calculated for RH/LH unit cells are 15.92 and −15.92°, respectively which gives a CRLH unit cell with the zero insertion phase.

In the case of an air filled medium ($\varepsilon_r = 1$, $\mu_r = 1$), the expressions of the inductances and the capacitances of the CRLH unit cell as a function of the permittivity and permeability, are such that

$$L_R = \mu_0 \Delta l; \quad L_L = \frac{1}{\omega^2 \varepsilon_0 \Delta l}$$
$$C_R = \varepsilon_0 \Delta l; \quad C_L = \frac{1}{\omega^2 \mu_0 \Delta l} \tag{20}$$

The variation of the CRLH refractive index according to the frequency given in Fig. 9 shows a zero refractive index at the resonant frequency f_0 = 1 GHz which can be deduced as the sum of the refractive indexes $n_{RH} = 1$ and $n_{LH} = -1$ of the RH/LH parts intervening in the CRLH unit cell realization.

As a first step to validate the WCIP method and verify the behavior of ZIM, we start by studying a transmission line which contains a ZIM part. There are two cases to treat this example. While in the first one we alternate asymmetric RH/LH unit cells to synthesize the ZIM medium. We use symmetric RH/LH unit cells in the second one as depicted in Fig. 10.

Yet, the Bloch impedances of symmetric RH/LH unit cells are purely real in the band pass delimited by the lower and upper cut-off frequencies of the LH and RH unit cells, respectively, as shown in Fig. 11. As a consequence, the propagating wave will not be attenuated after the ZIM region, as proved by the spatial variation of voltage shown in Fig. 12(b).

At 1 GHz, the RH/LH unit cells have insertion phases of 24 and −24°, respectively. The opposite insertion phases introduced by RH/LH unit cells can be clearly observed in the asymmetric case by the small undulations of the voltage through the ZIM region, as shown in Fig. 12(c).

The use of symmetric RH/LH unit cells to implement ZIM allows having an impedance matching between the various parts (Air, ZIM) of the analyzed circuits. Thus, we must have an electromagnetic wave propagation without attenuation after the ZIM region as shown in Fig. 12(b). Otherwise, with asymmetric RH/LH unit cells, we cannot maintain the matching condition. Therefore, an attenuation of the electromagnetic wave will be seen as shown in Fig. 12(c). In the case of ZIM-based asymmetric RH/LH unit cells, the voltage is measured at RH/LH unit cell's nodes alternatively. So, small undulations will happen on the ZIM region. But, when we have only one type of cell called CRLH unit cell, the insertion phase will be zero at each node and no undulations will be seen in this case.

In the following applications, we use symmetric unit cells to synthesize the ZIM medium, because we can match between the different cells since the characteristic impedance is purely real. After the theoretical explanation of the behavior of ZIM and how we use lumped element loaded microstrip transmission lines to generate them, we will illustrate the whole study by some applications highlighting the effectiveness of the WCIP method and the interest of the transmission line approach to synthesis ZIM. The next study will be based primarily on making interpretations starting from spatial distributions of voltage over the different circuits.

Applications

In all the following applications, we will consider an air filled medium matched with the ZIM medium. Thus, the calculated values of the lumped elements capacitors and inductors, at 1 GHz, are as the following: (C_R = 88.5 fF, L_R = 12.5 nH, C_L = 2.0 pF, L_L = 286 nH).

https://doi.org/10.1017/S175907871800168X Published online by Cambridge University Press

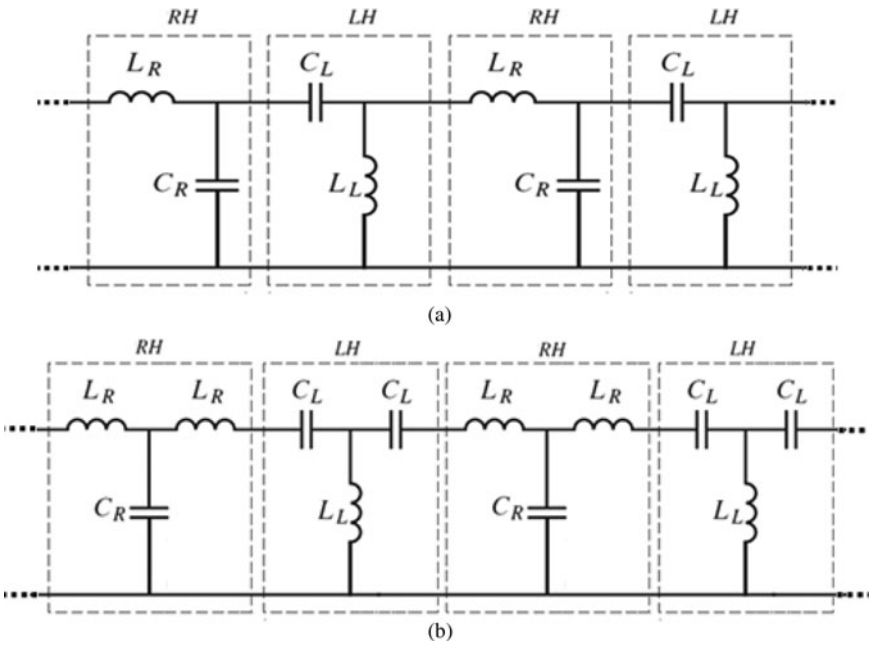

Fig. 10. Zero-index transmission line lumped models: (a) asymmetric RH/LH transmission line model and (b) symmetric RH/LH transmission line model.

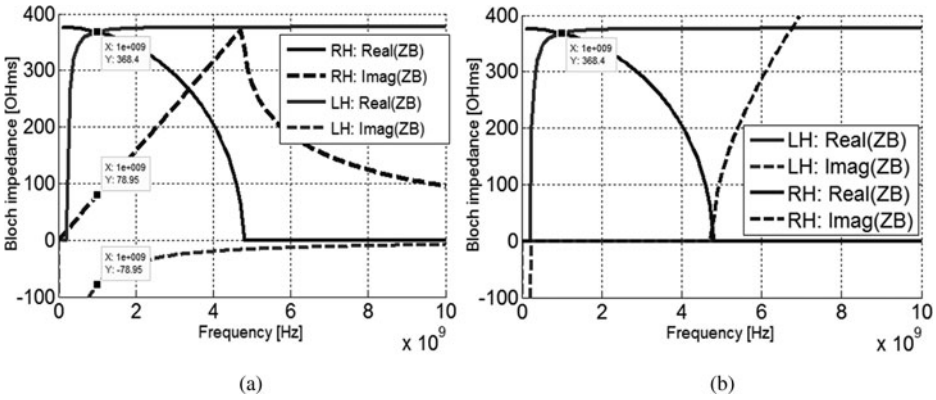

Fig. 11. Variation of the constant of propagation according to the frequency: (a) for asymmetric RH/LH unit cells and (b) for symmetric RH/LH unit cells.

Behavior of waveguides partially loaded with zero-index materials

Figure 13(a) shows a 2-D waveguide loaded with ZIM. The excitation is done on the left by a line of sources. The waveguide is charged by a line of adapted impedances.

From Fig. 13(b), we can clearly see that there is no variation of the magnitude of voltage through the ZIM region. A total transmission and super-reflection of electromagnetic waves can be obtained by coating a region embedded in the ZIM medium by perfect magnetic conductor (PMC) or perfect electric conductor (PEC) boundary, as shown in Figs 14(a) and 14(d). Since we have manipulated periodic lumped circuits, the PMC and PEC boundaries are satisfied by doing open and short circuit boundaries, respectively. From Fig. 14(b), we can observe that the incident electromagnetic waves can pass the PMC-coated object which is located inside the ZIM region without reflection (total transmission). The same result was obtained using COMSOL Multiphysics software as shown in Fig. 14(c). However, when the object is coated by the PEC boundary, a super-reflection of the incident plane wave is observed, as depicted by the simulation results shown in Figs 14(e) and 14 (f) and obtained with WCIP method and COMSOL Multiphysics software, respectively.

Effect of 2-D circular ZIM medium on the radiation of two embedded sources

First, two identical sources Sr_1 and Sr_2 are placed in free space, as shown in Fig. 15(a). We can detect from their radiation pattern a heterogeneous field distribution, which illustrates the interference phenomenon. The interference is constructive in a given position when the two emitted waves are in phase. However, the interference is destructive when the waves have phases with opposite signs. Second, the two sources are embedded in a circular ZIM region placed in free space as depicted in Fig. 15(b). We can clearly see a homogenous field distribution because all radiations exit the ZIM region with the same phase since there is no phase variation inside the metamaterial region.

To notice that all axes of voltage distribution are labeled according to the cell number. The right vertical scales designate the unit voltage.

https://doi.org/10.1017/S175907871800168X Published online by Cambridge University Press

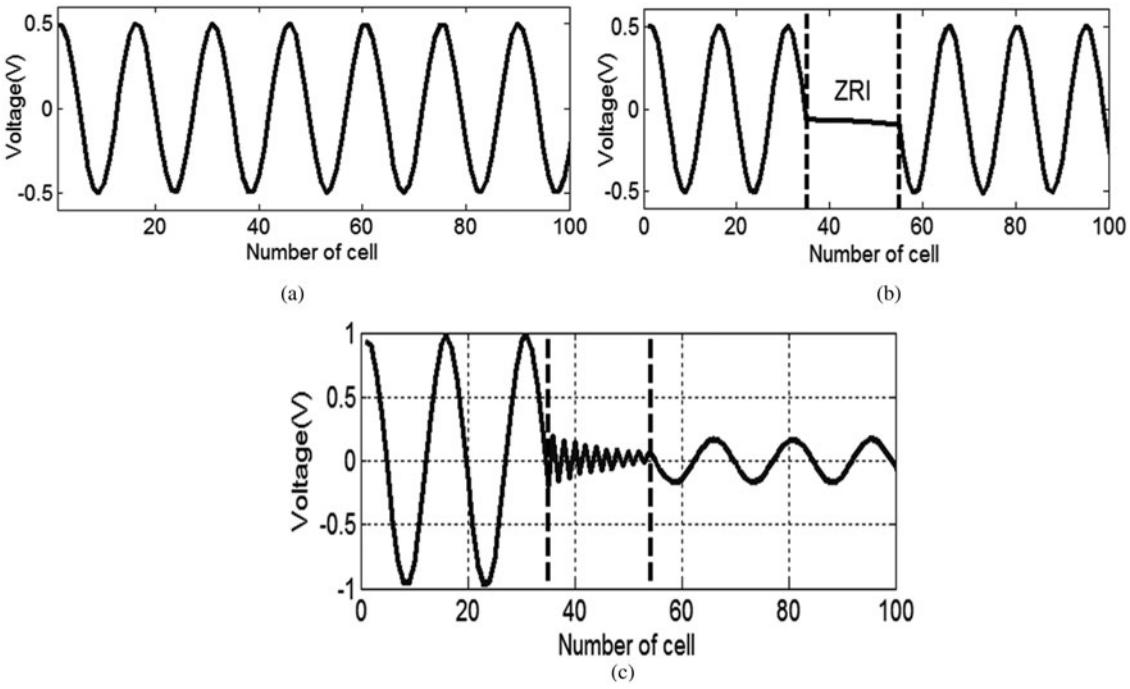

Fig. 12. Voltage distribution along the transmission line using WCIP method (the same curves were obtained by an ADS simulator): (a) a purely RH transmission line; (b) the ZIM region (delimited by dashed lines) implemented by symmetric RH/LH unit cells; and (c) the ZIM region implemented by asymmetric RH/LH unit cells.

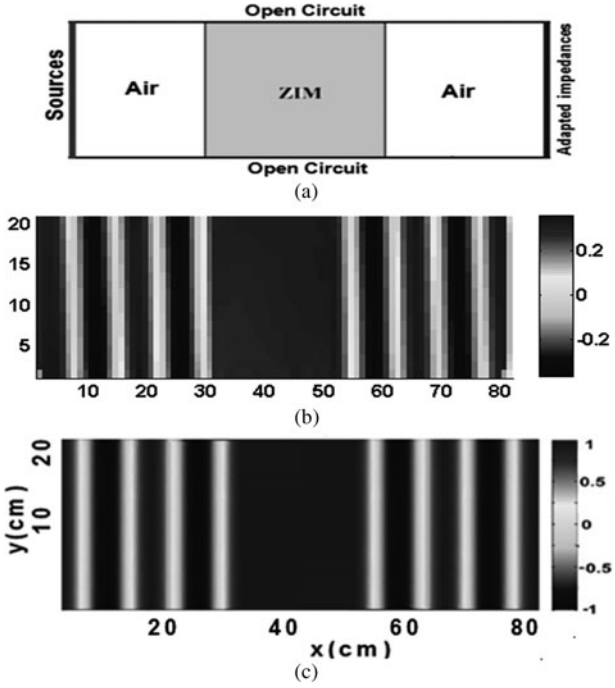

Fig. 13. (a) Schematic of a rectangular waveguide loaded with ZIM, (b) the voltage distribution using WCIP method, and (c) the electric field distribution using COMSOL Multiphysics.

Design of multi-beam antennas

If an electromagnetic source is placed inside a polygonal ZIM region embedded in a conventional dielectric medium, it will radiate into a number of directional beams equal to the number of sides of the peripheral boundary of the ZIM region [7].

Figure 16 shows the cases of triangular, square and hexagonal ZIM regions. We see that the electromagnetic source radiates into three, four, and six directional beams respectively. Thus, we can have a multi-beam antenna by choosing a polygonal peripheral ZIM layer.

Since the wavelength of the electromagnetic waves over ZIM media tends to infinity, many arbitrary embedded sources which initially have the same phase should interfere perfectly at all points in free space outside the ZIM region. We can use this characteristic to enhance the intensity of the electromagnetic field without perturbing the radiation pattern. This provides an interesting means to design antennas with enhanced far field radiation. Figures 17(a) and 17(b) show the voltage distribution through a ZIM square antenna, containing four sources.

When the electromagnetic waves exit the ZIM metamaterial region, they radiate in the form of plane waves from the surrounding space to the far-field space. In Fig. 17(c), we can clearly observe that the sources' radiations are perfectly combined outside the ZIM region. We can conclude that the use of ZIM permits to exhibit a perfect interference between many arbitrary located embedded sources without satisfying any particular interference condition.

Combination of the radiations of many sources embedded in ZIM on one focal point

Figure 18(a) shows an example of three point-sources located in arbitrary positions in the ZIM region. The frequencies of the three sources are the same in our simulations. The number of point sources in the ZIM region can be arbitrarily for both

https://doi.org/10.1017/S175907871800168X Published online by Cambridge University Press

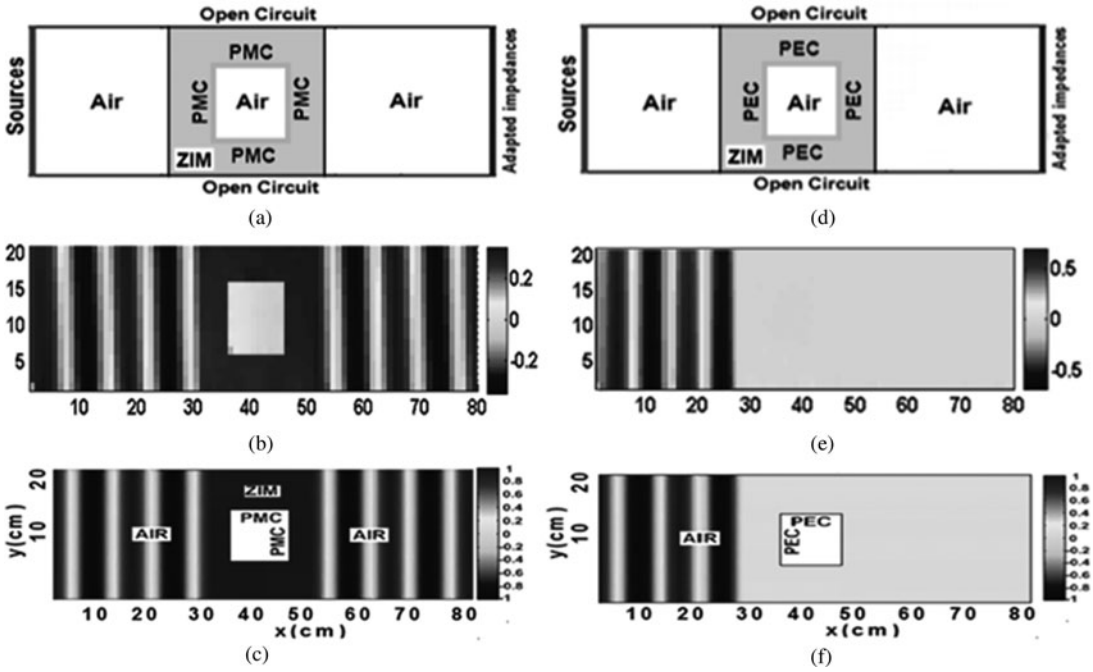

Fig. 14. (a) A waveguide which contains an air part coated with PMC boundary and its corresponding voltage distribution using WCIP method (b) and COMSOL Multiphysics (c); (d) a waveguide which contains an air part coated with PEC boundary and its corresponding voltage distribution using WCIP method (e) and COMSOL Multiphysics (f).

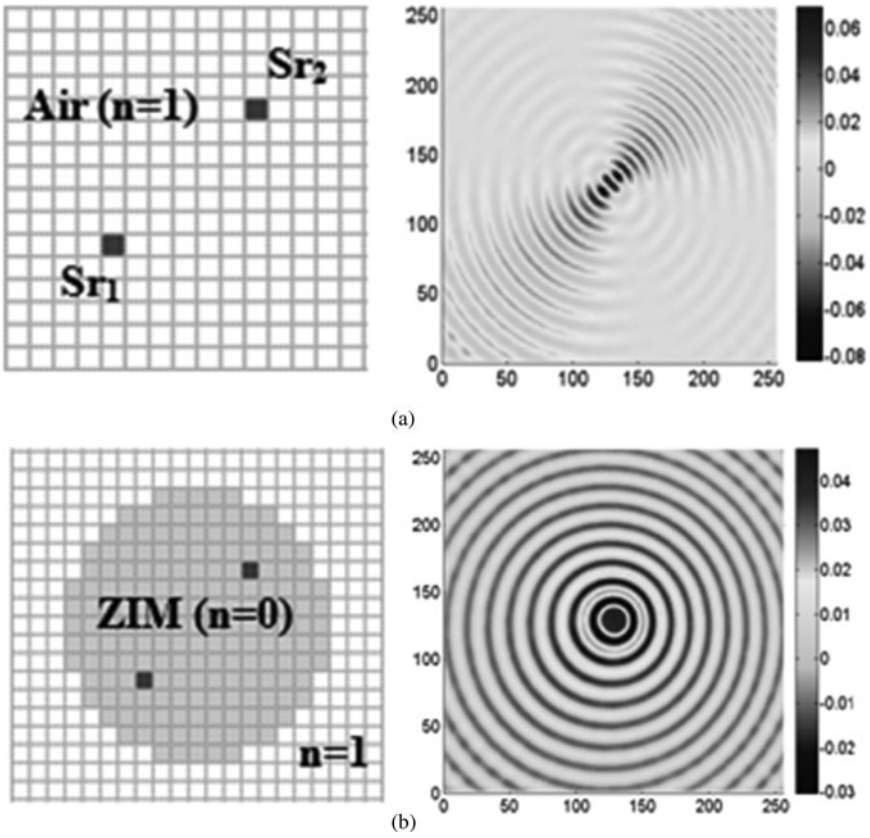

Fig. 15. (a) Two sources placed in free space and their corresponding spatial voltage distribution using WCIP method and (b) the two sources are embedded in a circular ZIM region.

https://doi.org/10.1017/S175907871800168X Published online by Cambridge University Press

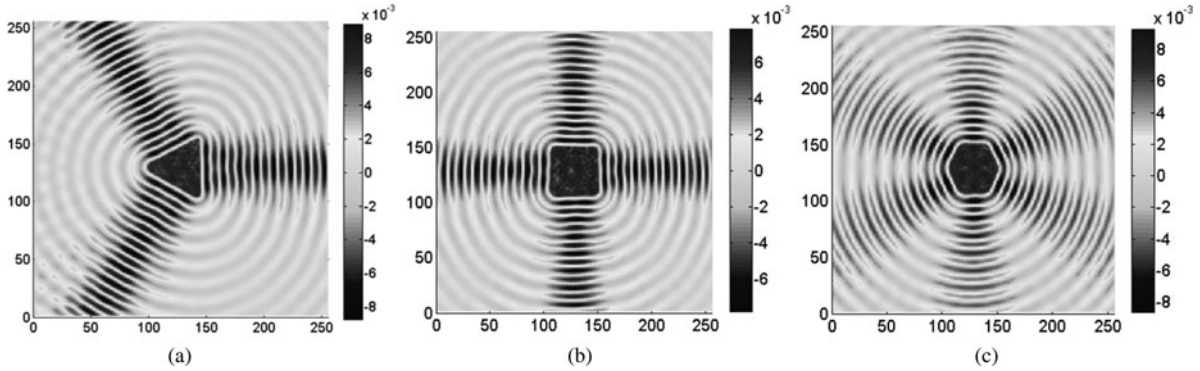

Fig. 16. Voltage distribution through the ZIM-based antennas with free-space using WCIP method: (a) triangular-shaped antenna, (b) square-shaped antenna, and (c) hexagonal-shaped antenna.

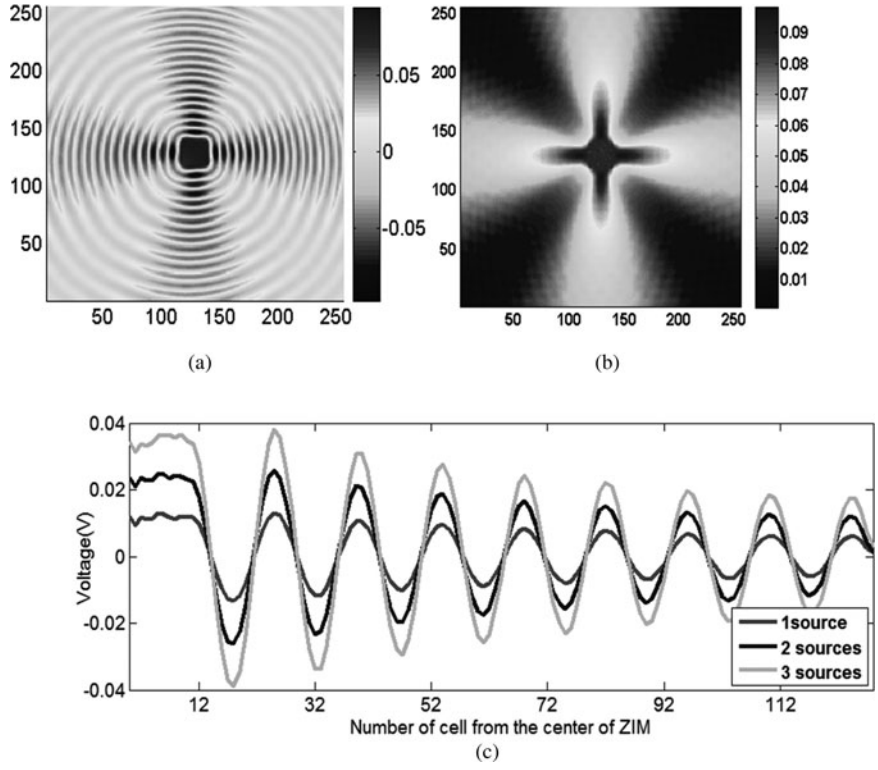

Fig. 17. Voltage distribution using WCIP method: (a) real (*Ez*) in volts, (b) abs (*Ez*) in volts, and (c) perfect combination of the sources' radiations outside the ZIM region.

positions and numbers. The focuser region can be with an arbitrary outer boundary.

From Fig. 18(c), we observe five focal points in the free space inner region of the focuser. Figure 18(d) shows that we can obtain a high voltage focal point at the center of the focuser by the addition of more sources inside the ZIM region. If the inner boundary of the focuser is circular, we will have a combination of all radiations in one focal spot at the center of the focuser. In fact, according to Snell's law, we can write the following equation:

$$n_{ZIM} \sin \theta_{ZIM} = n_{AIR} \sin \theta_{AIR} \tag{21}$$

According to (21), if the ZIM refractive index $n_{ZIM} = 0$ and the air refractive index $n_{AIR} \neq 0$, then sin θ_{AIR} should be zero, which gives an angle of refraction equal to zero in free space. In other words, when the radiation of a given source is incident on the interface between the ZIM and free space, the refractive angle should be zero. Therefore, for a circular inner boundary focuser, all radiations exiting the ZIM region to the free space region should be focused on one focal point at the center of the focuser as shown in Fig. 19.

A black circle is added in Fig. 19(b) to show the inner boundary of the circular focuser. ZIM can be used to exhibit a perfectly constructive interference independently of the locations of the embedded point sources. The above simulation results are convenient with the literature results depicted in [32].

Conclusion

In this paper, we have demonstrated how to use lumped element loaded transmission lines to synthesize ZIM. Then, we have

https://doi.org/10.1017/S175907871800168X Published online by Cambridge University Press

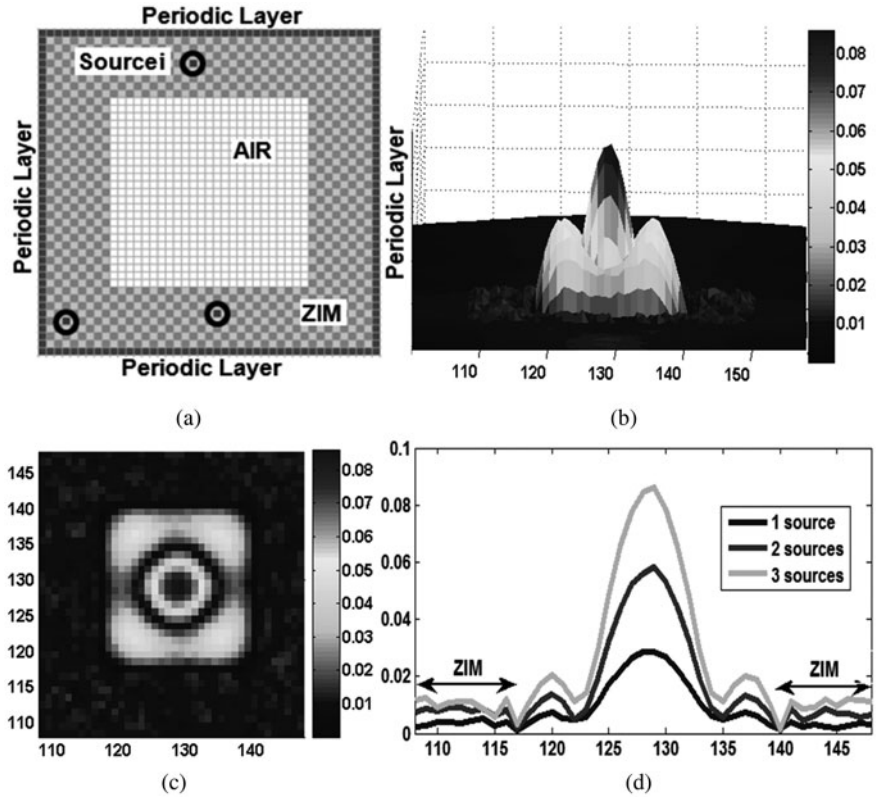

Fig. 18. (a) Simulating model of the electromagnetic focuser with square shaped inner boundary; (b) 3-D view of abs (*Ez*) through the focuser and (c) top view of abs (*Ez*) using WCIP method; and (d) focalization of the radiations of the sources on the center of the square focuser.

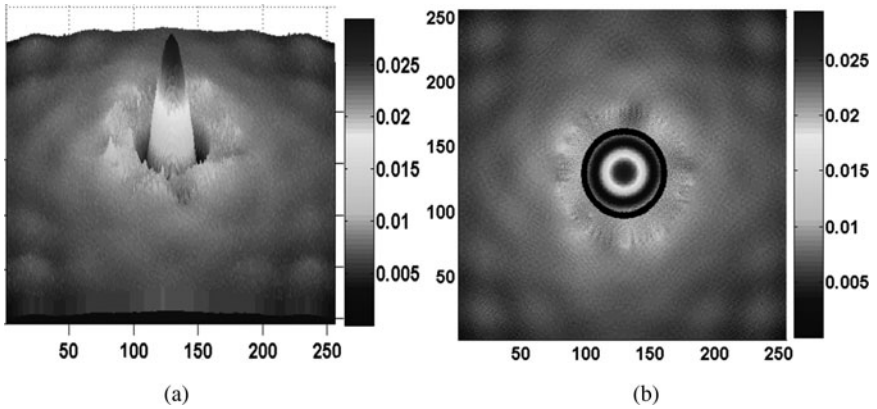

Fig. 19. (a) 3D-view and (b) top view of Abs (*Ez*) through the electromagnetic focuser with circular-shaped inner boundary using the WCIP method.

illustrated the whole theoretical study by applications highlighting the importance of ZIM, such as the design of multi-beam antennas, the perfect combination of many sources' radiations without any particular condition, and the transmission and the super reflection of electromagnetic waves inside waveguides partially loaded with ZIM. All simulations are carried out using an advantageous WCIP method suitable for this kind of electromagnetic problems.

References

1. **Veselago VG** (1968) The electrodynamics of substances with simultaneously negative values of ε and μ. *Soviet Physics Uspekhi* **10**, 509–514.
2. **Pendry JB** (2000) Negative refraction makes a perfect lens. *Physical Review Letters* **85**, 3966–3969.
3. **Sanada A, Caloz C and Itoh T** (2004) Planar distributed structures with negative refractive index. *IEEE Transactions on Microwave Theory and Techniques* **52**, 1252–1263.
4. **Kishor K, Baitha MN, Sinha RK and Lahiri B** (2014) Tunable negative refractive index metamaterial from V-shaped SRR structure: fabrication and characterization. *JOSA B* **31**, 1410–1414.
5. **Xu HX, Wang GM, Qing Qi M, Lv YY and Gao X** (2013) Metamaterial lens made of fully printed resonant-type negative-refractive-index transmission lines. *Applied Physics Letters* **102**, 193502.
6. **Grbic A and Eleftheriades GV** (2003) Growing evanescent waves in negative-refractive-index transmission-line media. *Applied Physics Letters* **82**, 1815–1817.
7. **He XT, Zhong YN, Zhou Y, Zhong ZC and Dong JW** (2015) Dirac directional emission in anisotropic zero refractive index photonic crystals. *Scientific Reports* **5**, 13085.
8. **Ding E, Wang Y, Liu X and Gong X** (2015) Waveguide splitting and squeezing in zero-index metamaterials embedded with defects. *AIP Advances* **5**, 107222.
9. **Silveirinha MG and Engheta N** (2012) Sampling and squeezing electromagnetic waves through subwavelength ultranarrow regions or openings. *Physical Review B* **85**, 085116.

https://doi.org/10.1017/S175907871800168X Published online by Cambridge University Press

10. **Zhang J, Luo Y and Mortensen NA** (2010) Transmission of electromagnetic waves through sub-wavelength channels. *Optics Express* **18**, 3864–3870.
11. **Edwards B, Alù A, Young ME, Silveirinha M and Engheta N** (2008) Experimental verification of epsilon-near-zero metamaterial coupling and energy squeezing using a microwave waveguide. *Physical Review Letters* **100**, 033903.
12. **Wu Y and Li J** (2013) Total reflection and cloaking by zero index metamaterials loaded with rectangular dielectric defects. *Applied Physics Letters* **102**, 183105.
13. **Xu Y and Chen H** (2011) Total reflection and transmission by epsilon-near-zero metamaterials with defects. *Applied Physics Letters* **98**, 113501.
14. **Liu R, Cheng Q, Hand T, Mock JJ, Cui TJ, Cummer SA and Smith DR** (2008) Experimental demonstration of electromagnetic tunneling through an epsilon-near-zero metamaterial at microwave frequencies. *Physical Review Letters* **100**, 023903.
15. **Cheng Q, Liu R, Huang D, Cui TJ and Smith DR** (2007) Circuit verification of tunneling effect in zero permittivity medium. *Applied Physics Letters* **91**, 234105.
16. **Ma HF, Shi JH, Cai BG and Cui TJ** (2012) Total transmission and super reflection realized by anisotropic zero-index materials. *New Journal of Physics* **14**, 123010.
17. **Lee WC and Chu TH** (2015) Modeling of a planar metamaterial power divider/combiner using transmission matrix method. *IEEE Microwave and Wireless Components Letters* **25**, 205–207.
18. **Caloz C, Ahn CH and Itoh T** (2005) Analysis 2D finite-size metamaterials by the transmission matrix method. In Antennas and Propagation Society International Symposium 3, 2–5.
19. **Siddiqui OF and Eleftheriades GV** (2011) Study of resonance-cone propagation in truncated hyperbolic metamaterial grids using transmission-line matrix simulations. *Journal of the Franklin Institute* **348**, 1285–1297.
20. **Elbellili T, Azizi MK, Latrach L, Trabelsi H and Baudrand H** (2018) Modeling and analysis of metamaterial lenses based on lumped circuits by using a wave concept iterative method. *International Journal of Microwave and Wireless Technologies* **10**, 253–263.
21. **Elbellili T, Azizi MK, Latrach L, Trabelsi H and Baudrand H** (2018) WCIP analysis of arbitrary shaped lumped metamaterial medium using a paint interface. In International Conference on Advanced Systems and Electric Technologies (IC_ASET), Tunisia.
22. **Elbellili T and Azizi MK** (2017) Study of perfect imaging by coupled negative refractive index lenses using WCIP method. In Internet of Things, Embedded Systems and Communications (IINTEC), Tunisia.
23. **Elbellili T, Azizi MK, Latrach L, Trabelsi H, Gharsallah A and Baudrand H** (2017) Characterization of the composite right/left-handed transmission line metamaterial circuits using iterative method WCIP. *International Journal of Microwave and Wireless Technologies* **9**, 1645–1652.
24. **Elbellili T, Azizi MK, Latrach L, Trabelsi H, Gharsallah A and Baudrand H** (2016) Analyzing of one dimensional quasi periodic circuit by using auxiliary sources in a WCIP method, Sciences of Electronics, Technologies of Information and Telecommunications (SETIT),Tunisia.
25. **Elbellili T, Azizi MK, Latrach L, Trabelsi H, Gharsallah A and Baudrand H** (2017) Analysis of planar microwave structures using transmission line-periodic lumped circuit by an iterative method WCIP. In Green Energy Conversion Systems (GECS), Tunisia.
26. **Azizi MK, Baudrand H, Latrach L and Gharsallah A** (2017) Metamaterial-Based Flat Lens: Wave Concept Iterative Process Approach. *Progress in Electromagnetics Research C* **75**, 13–21.
27. **Azizi MK, Baudrand H, Elbellili T and Gharsallah A** (2017) Almost periodic lumped elements structure modeling using iterative method: Application to photonic jets and planar lenses. *Progress in Electromagnetics Research M* **55**, 121–132.
28. **Azizi MK, Latrach L, Raveu N, Gharsallah A and Baudrand H** (2013) A new approach of almost periodic lumped elements circuits by an iterative method using auxiliary sources. *American Journal of Applied Sciences* **10**, 1457–1472.
29. **Fang K, Zhang Y, Li F, Jiang H, Li Y, Wang W and Chen H** (2012) Microwave collimation based on zero index metamaterials with Dirac point. *Optics Letters* **37**, 4654–4656.
30. **Eleftheriades GV, Grbic A and Antoniades M** (2004) Negative-refractive-index transmission-line metamaterials and enabling electromagnetic applications. In Antennas and Propagation Society International Symposium 2, 1399–1402.
31. **Garg R, Bahl I and Bozzi M** (2013) *Microstrip Lines and Slotlines*. Boston: Artech House.
32. **Zhai T, Shi J, Chen S, Liu D and Zhang X** (2011) Achieving laser ignition using zero index metamaterials. *Optics Letters* **36**, 2689–2691.

Mohamed Karim Azizi was born in Tunis, Tunisia, on December 26, 1979. He received his M.Sc. degree in Telecommunications from SupCom in 2008. He received his Ph.D. degree in Electronics from the Faculty of Sciences of Tunis, Tunisia in 2013. He is currently an associated Professor in the Department of Computer Sciences in The Higher Institute of Multimedia Arts of Mannouba, ISAMM, Tunisia. His research interest at present includes metamaterials, metasurfaces, and graphene antennas.

Taieb Elbellili was born in Kasserine, Tunisia, on April 29, 1980. He received his M.Sc. degree in Electronic systems from the Faculty of Sciences of Tunis, Tunisia in 2006. Since 2015, he has been working toward his Ph.D. His research focuses on computational electromagnetic methods for metamaterial modeling.

Henri Baudrand (SM'90–F'04–LF'14) received his Ph.D. degree in microwaves from the Institut National Polytechnique, Toulouse, France, in 1966. He is a Professor Emeritus with the Ecole Supérieure d'Electronique Electrotechnique Informatique, ENSEEIHT, National Polytechnic Institute of Toulouse, Toulouse, France. He has authored and coauthored six books: Introduction au calcul des éléments de circuits microondes, optimisation des circuits non linéaires, calcul des circuits microondes par les schémas équivalents (CEPADUES Editions Toulouse), New Trends and Concept in Microwave Theory and Technics, Adaptation de la méthode WCIP aux circuits SIW et SINRD: WCIP: Wave Concept Iterative Process, and Modélisation Globale des Circuits Electroniques Hautes Fréquences. He cosigned over 110 publications in journals, four chapters in scientific books, and 250 communications in international conferences. He is a Fellow Member of "Electromagnetism Academy" and Senior Member of IEE Society. He was President of URSI France Commission B for 6 years (1993–1999), the IEEE-MTT-ED French chapter (1996–1998), and the International Comity of O.H.D. (Hertzian Optics and Dielectrics) between 2000 and 2004. He was the recipient of Officier des Palmes académiques and Doctor Honoris causa of lasi University (1996).

Hichem Trabelsi was born in Tunisia, in 1962. He received his Ph.D. in Electronics from the University of Pierre & Marie Curie, Paris VI, France in 1991. He joined the Department of Physics at the Faculty of Sciences, Tunis, in 1992, where he is currently working on microwave active and passive filters and electromagnetic theory for solving field problems in microwave circuits.

https://doi.org/10.1017/S175907871800168X Published online by Cambridge University Press